Hindawi Publishing Corporation
Journal of Nanomaterials
Volume 2016, Article ID 4261069, 7 pages
http://dx.doi.org/10.1155/2016/4261069

Research Article

Facile Solution Route to Synthesize Nanostructure $Li_4Ti_5O_{12}$ for High Rate Li-Ion Battery

M. V. Tran,[1] N. L. T. Huynh,[2] T. T. Nguyen,[3] D. T. C. Ha,[1] and P. M. L. Le[1,2]

[1]*Department of Physical Chemistry, VNUHCM-University of Science, 227 Nguyen Van Cu Street, District 5, Ho Chi Minh City, Vietnam*
[2]*Applied Physical Chemistry Laboratory, Faculty of Chemistry, VNUHCM-University of Science, 227 Nguyen Van Cu Street, District 5, Ho Chi Minh City, Vietnam*
[3]*College of Science, Can Tho University, Ninh Kieu District, Can Tho City, Vietnam*

Correspondence should be addressed to P. M. L. Le; lmlphung@hcmus.edu.vn

Received 28 September 2016; Accepted 21 November 2016

Academic Editor: Zheng Zhang

High rate Li-ion batteries have been given great attention during the last decade as a power source for hybrid electric vehicles (HEVs, EVs, etc.) due to the highest energy and power density. These lithium batteries required a new design of material structure as well as innovative electrode materials. Among the promising candidates, spinel $Li_4Ti_5O_{12}$ has been proposed as a high rate anode to replace graphite anode because of high capacity and a negligible structure change during intercalation of lithium. In this work, we synthesized a spinel $Li_4Ti_5O_{12}$ in nanosize by a solution route using LiOH and $Ti(OBu)_4$ as precursor. An evaluation of structure and morphology by XRD and SEM exhibited pure spinel phase $Li_4Ti_5O_{12}$ and homogenous nanoparticles around 100 nm. In the charge-discharge test, nanospinel $Li_4Ti_5O_{12}$ presents excellent discharge capacity 160 mAh/g at rate C/10, as well as good specific capacities of 120, 110, and 100 mAh/g at high rates C, 5C and 10C, respectively.

1. Introduction

Since the first investigation of lithium's intercalation by Colbow et al. in 1989 [1], spinel $Li_4Ti_5O_{12}$ has become one of attractive anode materials for Li-ion battery application because of nontoxic, inexpensive, thermal stability and negligible changed volume cell during charge-discharge cycling with a specific capacity of approximately 175 mAh/g [2, 3]. The process of reversible intercalation occurs around 1.55 V (versus Li^+/Li), which is higher than its of lithiated graphite (below 1 V) to avoid the formation of unstable solid electrolyte interface (SEI) [1, 4, 5]. Despite these advantages, the inconveniences still exist in spinel phase $Li_4Ti_5O_{12}$ such as a low electronic conductivity and a poor lithium diffusion rate which limited its application in high rate Li-ion batteries [6, 7]. To overcome these problems, nanoscale particles size or 1D–3D nanostructure of $Li_4Ti_5O_{12}$ (nanowires, nanosheets, nanoparticles, nanotubes, nanorods, and microspheres) has been proposed to improve the electrochemical performances (higher specific capacity, high rate capability, and good charge-discharge cycling stability) due to shortening the diffusion way of lithium [8–14]. Table 1 summarized the highlighted results of $Li_4Ti_5O_{12}$ reported in the literature.

The remarkable results are mostly reported for using hydrothermal synthesis pathway with strictly controlled parameters such as temperature and pressure. However, these conditions are quite difficult for large scale application in the industry.

In this work, we report a facile solution way to synthesize nanospinel $Li_4Ti_5O_{12}$ through the formation of intermediate C-base centered orthorhombic $Li_{1.81}H_{0.19}Ti_2O_5{\cdot}2H_2O$ (LTH). The presence of LTH seems to be easily converted in $Li_4Ti_5O_{12}$ phase at low temperature range (<700°C) compared to the same layered structure α/β-Li_2TiO_3, usually obtained in solid state reaction or hydrothermal process [15]. Nanospinel $Li_4Ti_5O_{12}$ synthesized is investigated by charge-discharge test at high rate 1C to 10C. The diffusion coefficient of lithium ions (D_{Li}) in the host $Li_4Ti_5O_{12}$ can be also determined by cyclic voltammetry.

Table 1: Summarizing different synthetic methods of nanoscale/nanostructure $Li_4Ti_5O_{12}$ reported in the literature.

Methods	Temperature	Scale	Morphology	Specific capacity	Ref
Sol-gel + pyrolysis step	25°C; 800°C	Nanoparticles, 5–400 nm	Versatile morphologies	142 mAh/g (C/10) 126 mAh/g (0.2C)	[14]
Hydrothermal/ + pyrolysis	400°C (300 bar) 700°C (24 h)	Nanoparticles, 150–200 nm	Versatile morphologies	140 mAh/g (10C)	[16]
Solvothermal + pyrolysis	235°C (16 h) 500°C (3 h)	Nanoparticles, 10–20 nm	Versatile morphologies	154 mAh/g (C/10)	[17]
Two-step process in solution	120°C (2 h) 120°C in 10 M NaOH	1D structure, tube, 6–11 nm	Nanotube	156 mAh/g (C/10) 145 mAh/g (2C)	[18]
Hydrothermal in 10 M NaOH	180°C 500–800°C	1D structure, tube, 6–11 nm	Nanorod	147.5 mAh/g (2.5C)	[29]
Solvothermal in $Li(OH)\cdot H_2O$	180°C 500–800°C	1D structure, tube, 130 nm in diameter	Nanowire	128 mAh/g (10C)	[30]

2. Experimental

For the preparation of nanostructured $Li_4Ti_5O_{12}$, 7 mL solution of $Ti(OBu)_4$ ($d = 1.491$ g/mL at 20°C, $M = 340{,}39$ g/mole) was added dropwise into 25 mL solution of LiOH 1 M solution under vigorous stirring at 4–6°C and the ratio of Li : Ti was 1 : 1.33. The low temperature is required to keep the hydrolyze process of $Ti(OBu)_4$ occurring slowly for limitation of TiO_2 rutile. Thus, the expected intermediate is certainly pure without emerging TiO_2 rutile, the as-prepared powder was collected through a centrifuge and washed many times with deionized water to neutral pH. The as-prepared powders were aged in the air by two steps: at 100°C for 36 hours to form C-base centered orthorhombic $Li_{1.81}H_{0.19}Ti_2O_5\cdot 2H_2O$ (LTH). The intermediate phase was calcined at 600°C for 6 hours in the air to transfer to the spinel phase of $Li_4Ti_5O_{12}$.

The sample was identified by X-Ray Diffraction (XRD) performed with a D8-Advance (Bruker) diffractometer using CuKα radiation ($\lambda_{K\alpha} = 1.5408$ Å). XRD pattern was collected in the range 10–70° (0.029°/s). Lattice parameters were calculated by software Celref. The Raman spectra were measured with a LaBRAM HR 800 (Jobin-Yvon-Horiba) Raman microspectrometer, using a He:Ne laser (632.8 nm) as the excitation source. The morphology and the distribution of grain size were determined by using Scanning Electron Microscope (FE-SEM S4800 Hitachi, Japan).

The electrode paste was prepared by mixing of $Li_4Ti_5O_{12}$ with acetylene black and polytetrafluoroethylene (PTFE) at a weight ratio of 80 : 15 : 5. The paste was laminated to 0.1 mm thickness, cut into pellets with a diameter of 10 mm, and dried at 130°C under a vacuum in 24 hours. The electrochemical properties of nanocrystalline $Li_4Ti_5O_{12}$ were evaluated by the cyclic voltammetry (CV) and the charge-discharge test at a various rate (from C/10 to 10C) in Swagelok cells. The cyclic voltammetry (CV) of nanospinel $Li_4Ti_5O_{12}$ has been performed in potential range of 1–2.5 V (versus Li^+/Li) in the various rates from 10 μV/s to 100 μV/s. An electrode $Li_4Ti_5O_{12}$ and Li foil were used as the positive and negative materials in the half-cell and a solution of 1 M $LiPF_6$ in a mixture of ethylene carbonate (EC) and dimethyl carbonate (DMC) at a ratio of EC : DCM = 2 : 1 was used as the electrolyte.

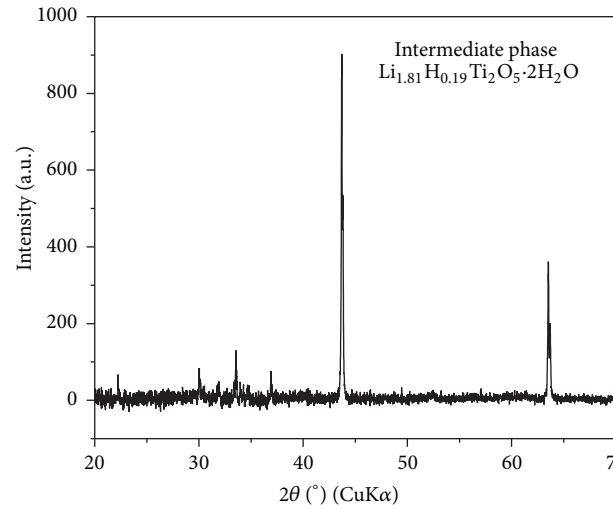

Figure 1: XRD pattern of intermediate phase $Li_{1.81}H_{0.19}Ti_2O_5\cdot 2H_2O$.

3. Results and Discussion

3.1. Structure and Morphology. The formation of intermediate C-base centered orthorhombic $Li_{1.81}H_{0.19}Ti_2O_5\cdot 2H_2O$ was determined by XRD patterns as shown in Figure 1. According to previous studies [1, 2, 12], structure of $Li_4Ti_5O_{12}$ is a cubic spinel (unit cell parameter around 8.36 Å) with space group of F3dm and can be represented as $[Li_3]^{8a}[Li_1Ti_5]^{16d}[O_{12}]^{32e}$. Most of ions Li^+ are situated at the tetrahedral 8a site, while the rest of ion Li^+ and ions Ti^{4+} occupy randomly the octahedral 16d sites with a ratio of 1 : 5; and the oxygen atoms totally are located at the 32e site. As shown in Figure 2, the XRD patterns of sample could be identified to a pure phase of spinel $Li_4Ti_5O_{12}$ (JCPDS: 49-0207) [2, 13]. The broadening of diffraction peaks was related to the nanoparticles size. The lattice parameter of $Li_4Ti_5O_{12}$ was evaluated by seven diffraction peaks and calculated to be $a = 8.3564$ Å (±0.0172 Å). This value was in good agreement with the published results [2, 14, 16–18].

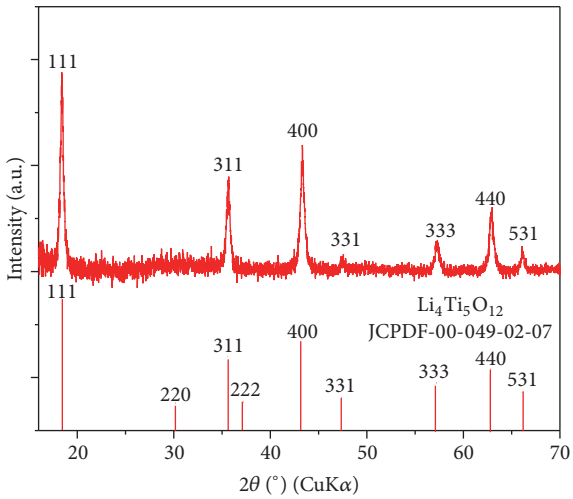

FIGURE 2: XRD pattern of nanospinel $Li_4Ti_5O_{12}$ with JCPDF 49-0207 [13].

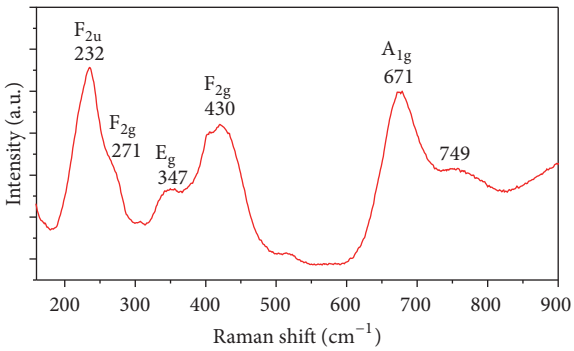

FIGURE 3: Raman scattering spectra of $Li_4Ti_5O_{12}$.

Despite a heat treatment at 600°C in the last step, the peaks of XRD pattern were still quite large. It is considered that the sample was crystallized in small particle sizes. According to the Debye-Scherrer formula (1), the average size of particles was calculated from the full width of half maximum (FWHM) of diffraction peaks.

$$d_{hkl} = \frac{k\lambda}{\beta \cos\theta}, \quad (1)$$

where d_{hkl} is the average size, k is the constant depending on the crystallite shape (0.9), λ is the wavelength of copper Kα X-ray radiation (1.5406 Å), β is the FWHM of the most intense peak, and θ is the diffraction angle. The size reached around 40 nm. The nanosize of particles will suggest a fast kinetic of intercalation of lithium ion due to shortening the way diffusion [6, 7].

Following the theoretical calculation of $A[B_2]O_4$ spinel-type compound, spinel phase $Li_4Ti_5O_{12}$ consists of a symmetric group $O^7{}_h$ with the five expected F_{2g}, E_g, A_{1g} Raman active vibration [19–22]. The Raman spectrum of nanostructure was shown in Figure 3 in the region of wave number between 150 and 900 cm^{-1}. In the high frequency, two modes at 671 cm^{-1} and 740 cm^{-1} (vibration mode A_{1g}) were assigned to the vibrations of Ti–O bonds in $[TiO_6]$ octahedra, while the stretching vibrations of the Li–O bonds in $[LiO_4]$ and $[LiO_6]$ polyhedra were characterized by two modes in region medium frequency 430 cm^{-1} and 374 cm^{-1}, respectively. Two last modes in low frequency were attributed to the bending vibrations of O–Ti–O bonds (235 cm^{-1}) and O–Li–O bonds (160 cm^{-1}). These Raman spectra features were similar to those reported by Julien et al. [19].

The SEM and TEM images of nanostructure $Li_4Ti_5O_{12}$ in Figure 4 indicated particles shape mostly like a rod and its size fell into the nanometric scale around 100 nm. A good distribution and nanoparticle size were in good coherence with large XRD peaks.

3.2. Electrochemical Properties. The spinel phase $Li_4Ti_5O_{12}$ can insert/extract electrochemically 3 Li^+ ions per mole reversibility in the potential 1.55 V (versus Li^+/Li) causing the reduction of couple redox Ti^{4+}/Ti^{3+} within a specific capacity theoretical of 175 mAh/g [1]. The process of intercalation of lithium ions seems to be a two-phase mechanism, similar to the olivine $LiFePO_4$ [23, 24]. All intercalating lithium ions inserted into the 16c octahedral site and the lithium ions initial in the tetrahedral 8a site moved simultaneously to the 16c octahedral site. Hence, the route diffusion of lithium ions into spinel $Li_4Ti_5O_{12}$ can be represented following the pathway 16c–8a–16c. The fully discharged compound can be described as $[Li_6]^{16c}[LiTi_5]^{16d}[O_{12}]^{32e}$ [25, 26]. In particular, the lithiation/delithiation of this spinel accompanies a "zero strain" characteristic; it means that lattice parameter of $Li_4Ti_5O_{12}$ remained constant between the initial state of $Li_4Ti_5O_{12}$ and the final state of $Li_7Ti_5O_{12}$ [2, 3, 14].

The electrochemical performance of nanospinel $Li_4Ti_5O_{12}$ synthesized has been investigated by cyclic voltammetry (CV) within 1–2.5 V (versus Li^+/Li) and galvanostatic cycling within 1–2.5 V (versus Li^+/Li). As shown in Figure 5(a), a symmetric couple redox peak was observed in 1.50 V (peak cathode) and 1.60 V (peak anode), corresponding to a reaction of couple redox Ti^{4+}/Ti^{3+} at lowest rate 10 μV/s. A sharp form of two peaks characterized a two-phase mechanism of lithium insertion and related to a large plateau voltage (~1.55 V versus Li^+/Li) in galvanostatic curves charge-discharge [24, 26]. Figure 5(a) also exhibited the evolution of CV curves of nanospinel $Li_4Ti_5O_{12}$ in the various rate from 10 μV/s to 100 μV/s. Following the increase of scan rate, it could be noticed that peak's position shifted around 300 mV in highest rate 100 μV/s and the redox peaks broadened gradually. The diffusion coefficient of lithium ions (D_{Li}) in the host $Li_4Ti_5O_{12}$ electrode can be determined from a linear relationship between peak currents (I_p) and the square root of the scan rate ($v^{1/2}$) from the CV curves, according to the following Randles-Sevcik equation (2) [27]:

$$I_p = 2.60 \times 10^5 n^{3/2} A D_{Li}^{1/2} C_{Li} v^{1/2}, \quad (2)$$

where I_p is the peak current, A is the surface area of electrode (0.785 cm^2), n is the number of electrons transfer per molecule ($n = 1$), C_{Li} is the concentration of lithium ion

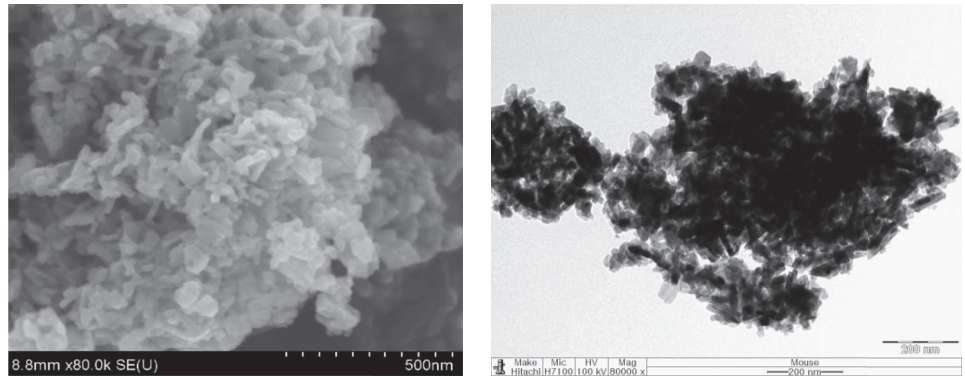

(a) (b)

FIGURE 4: SEM image (a) and TEM image (b) of nanoscale $Li_4Ti_5O_{12}$ powder.

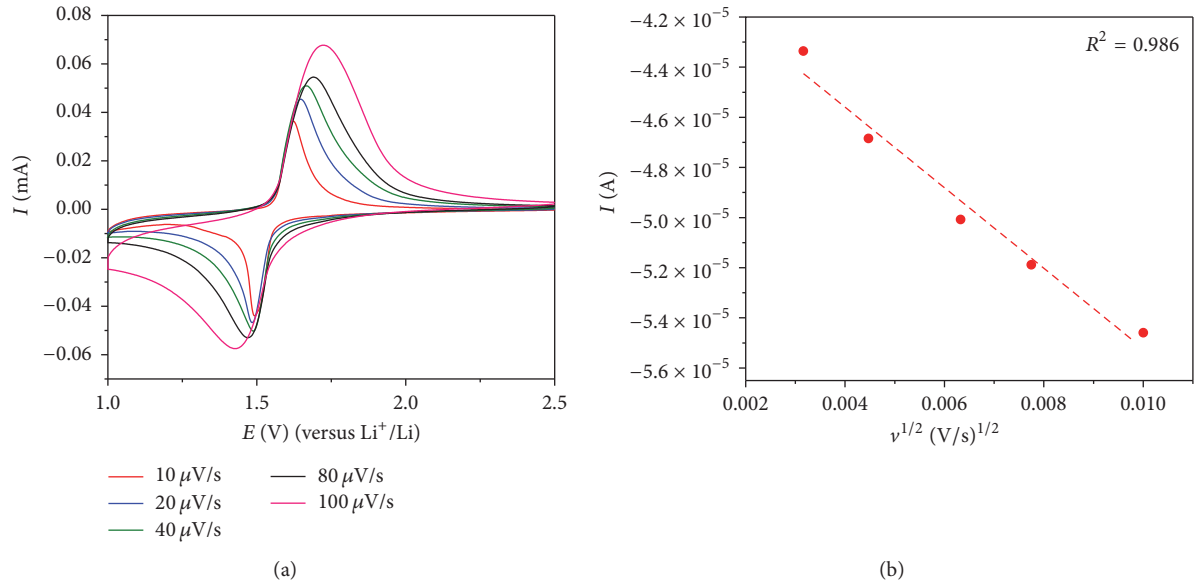

(a) (b)

FIGURE 5: (a) Evolution of CV curves in the various rate from 10 μV/s to 200 μV/s and (b) I_{pc} as a function of the square root of the scan rate $v^{1/2}$.

in $Li_4Ti_5O_{12}$ electrode, v is scan rate, and D_{Li} is the diffusion coefficient of lithium ions.

It can be seen from Figure 5(b) in the plots of I_p as a function of the square root of the scan rate ($v^{1/2}$) that a good linear relation I_p between I_p and $v^{1/2}$ was observed. The diffusion coefficient of lithium ions was found to be 3.8×10^{-12} cm^2/s, which was in accord with other authors' results [6, 7].

Discharge-charge profiles of spinel $Li_4Ti_5O_{12}$ could be described by three regions: a quick drop of voltage corresponding to a region of solid solution with a content of lithium below 0.2, a main region of two-phase mechanism displayed by a plateau voltage in 1.55 V, and other solid solution region after plateau voltage [2, 14, 23]. The discharge-charge profiles in 1st cycle of nanospinel $Li_4Ti_5O_{12}$ at rate C/10, 1C, and 10C were shown in Figure 6(a). The curve in rate 1C seems to quasi-superimpose onto its rate C/10 without polarization, while huge polarization around 150 mV was observed in the curve in rate 10C. The polarization brought about shortening of plateau voltage in 1.4 V and decreased a content of lithium ion inserted. In the first cycle, nanospinel $Li_4Ti_5O_{12}$ could insert 3 Li^+ ions at C/10, 2.6 at 1C, and 2.3 at 10C corresponding to a specific capacity of 175 mAh/g, 150 mAh/g, and 110 mAh/g, respectively [28]. Figures 6(b) and 6(c) presented the typical curves of discharge-charge at 1C and 10C. At the high rate, an excellent performance of nanospinel $Li_4Ti_5O_{12}$ was observed, in spite of the gradual decrease of lithium ion amount intercalated after some decade cycles. After 100 cycles (Figure 6(d)), the remaining capacities were 86% (rate C/10), 74% (rate 1C), and 75% (rate 10C) of capacity initial that were registered, corresponding to a specific capacity of 150 mAh/g, 111 mAh/g, and 100 mAh/g, respectively. We believe that the particles in nanosize shorten the pathway diffusion of lithium ions and encourage the performance of spinel $Li_4Ti_5O_{12}$ synthesized during the high rate capability test. These results are comparable with

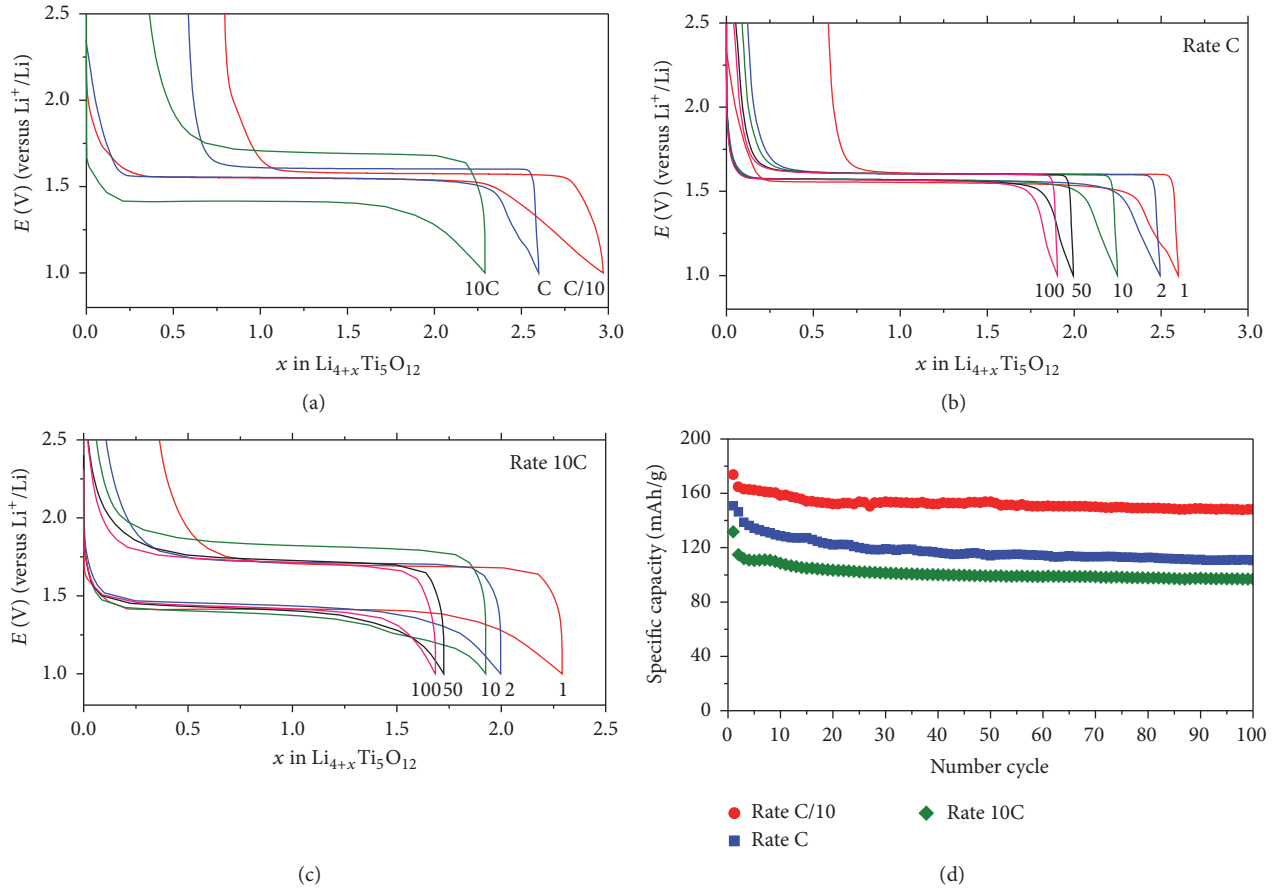

FIGURE 6: Charge-discharge of nano-$Li_4Ti_5O_{12}$ in the potential range 1–2.5 V (versus Li^+/Li) (a) cycle 1 at rate C/10, C, and 10C; (b) typical curves at rate 1C; (c) typical curves at rate 10C; and (d) specific capacity versus number of cycles.

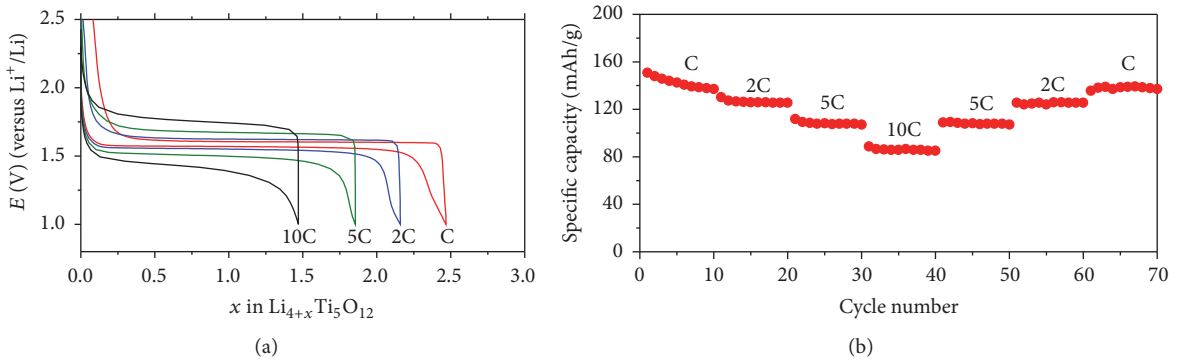

FIGURE 7: (a) Charge-discharge curves of nano-$Li_4Ti_5O_{12}$ in the potential range 1–2.5 V (versus Li^+/Li) in high rate 1C to 10C and (b) evolution specific capacity as a function of cycles and charge-discharge rates.

the previous studies which showed a specific capacity of 150 mAh/g in rate 1C and 100 mAh/g in rate 10C [9, 11, 15].

The rate capability of charge-discharge test from 1C to 10C was shown in Figure 7. Whatever the rate, a remarkable stability is obtained and the discharge-charge curves show clearly the effect of polarization to a decrease of specific capacity. The capacity obtained was 150 mAh/g at 1C, 130 mAh/g at 2C, 120 mAh/g at 5C, and 98 mAh/g at 10C. The specific capacity and cycling stability are comparably equal to these values obtained for 1D–3D nanostructure $Li_4Ti_5O_{12}$ synthesized by hydrothermal, solvothermal, electrospinning, and so forth [17, 18, 29, 30]. In the high rate performance, the electrode polarization was absolutely controlled by the limitation of internal resistance (ohmic drop), charge transfer, and mass transfer. Hence, the performance at high rate of nanospinel $Li_4Ti_5O_{12}$ would require an optimization of the electrode

formation process, typically using a composite of spinel and high conductivities matrix carbon like CNTs or graphene [28, 31, 32].

4. Conclusions

This study has showed a facilitated route to synthesize nanospinel $Li_4Ti_5O_{12}$ through intermediate phase. The nanospinel had good distribution grains and the average of particles was around 100 nm. The diffusion coefficients of lithium ions determined from CV curves reached 3.8×10^{-12} cm^2/s. In a high rate of charge-discharge, an excellent electrochemical performance of nanospinel was observed and the specific capacities of 110 mAh/g and 100 mAh/g were achieved at 1C and 10C rate, respectively. The rate capability test showed a relation between a specific capacity and electrode polarization. Further studies regarding the role of CNTs or graphene could increase electronic conductivities electronic of electrode to improve the performance of this spinel phase.

Competing Interests

The authors declare that they have no competing interests.

Acknowledgments

This research is funded by Vietnam National University Ho Chi Minh City (VNU-HCM) under Grants HS2013-76-01 and TX2016-18-04. The authors would like to thank Office of Naval Research Global (ONRG) for Grant N62909-13-1-N235.

References

[1] K. M. Colbow and R. R. Dahn Haering Jr., "Structure and electrochemistry of the spinel oxides $LiTi_2O_4$ and $Li_4/_3Ti_5/_3O_4$," *Journal of Power Sources*, vol. 26, no. 3-4, pp. 397–402, 1989.

[2] T. Ohzuku, A. Ueda, and N. Yamamoto, "Zero-strain insertion material of $Li[Li_{1/3}]Ti_{5/3}O_4$ for rechargeable lithium cells," *Journal of the Electrochemical Society*, vol. 142, no. 5, pp. 1431–1435, 1995.

[3] K. Ariyoshi, R. Yamato, and T. Ohzuku, "Zero-strain insertion mechanism of $Li[Li_{1/3}Ti_{5/3}]O_4$ for advanced lithium-ion (shuttlecock) batteries," *Electrochimica Acta*, vol. 51, no. 6, pp. 1125–1129, 2005.

[4] D. Guerard and A. Herold, "Intercalation of lithium into graphite and other carbons," *Carbon*, vol. 13, no. 4, pp. 337–345, 1975.

[5] Y. F. Reynier, R. Yazami, and B. Fultz, "Thermodynamics of lithium intercalation into graphites and disordered carbons," *Journal of the Electrochemical Society*, vol. 151, no. 3, pp. A422–A426, 2004.

[6] T.-F. Yi, S.-Y. Yang, and Y. Xie, "Recent advances of $Li_4Ti_5O_{12}$ as a promising next generation anode material for high power lithium-ion batteries," *Journal of Materials Chemistry A*, vol. 3, no. 11, pp. 5750–5777, 2015.

[7] B. Zhao, R. Ran, M. Liu, and Z. Shao, "A comprehensive review of $Li_4Ti_5O_{12}$-based electrodes for lithium-ion batteries: the latest advancements and future perspectives," *Materials Science and Engineering R: Reports*, vol. 98, pp. 1–71, 2015.

[8] A. Guerfi, S. Sévigny, M. Lagacé, P. Hovington, K. Kinoshita, and K. Zaghib, "Nano-particle $Li_4Ti_5O_{12}$ spinel as electrode for electrochemical generators," *Journal of Power Sources*, vol. 119–121, pp. 88–94, 2003.

[9] J. Kim and J. Cho, "Spinel $Li_4Ti_5O_{12}$ nanowires for high-rate li-ion intercalation electrode," *Electrochemical and Solid-State Letters*, vol. 10, no. 3, pp. A81–A84, 2007.

[10] Y. Qiao, X. Hu, Y. Liu, and Y. Huang, "$Li_4Ti_5O_{12}$ nanocrystallites for high-rate lithium-ion batteries synthesized by a rapid microwave-assisted solid-state process," *Electrochimica Acta*, vol. 63, pp. 118–123, 2012.

[11] H.-C. Chiu and G. P. Demopoulos, "A novel green approach to synthesis of nanostructured $Li_4Ti_5O_{12}$ anode material," *ECS Transactions*, vol. 50, pp. 119–126, 2013.

[12] E. Ferg, R. J. Gummow, A. de Kock, and M. M. Thackeray, "Spinel anodes for lithium-ion batteries," *Journal of the Electrochemical Society*, vol. 141, no. 11, pp. L147–L150, 1994.

[13] D. Tsubone, T. Hashimoto, K. Igarashi, and T. Shimizu, "Electrical characterization of phase changes in lithium titanate," *Journal of the Ceramic Society of Japan*, vol. 102, pp. 180–184, 1994.

[14] S. Bach, J. P. Pereira-Ramos, and N. Baffler, "Electrochemical properties of sol-gel $Li_{4/3}Ti_{5/3}O_4$," *Journal of Power Sources*, vol. 81-82, pp. 273–276, 1999.

[15] I. Veljković, D. Poleti, L. J. Karanović, M. Zdujić, and G. Branković, "Solid state synthesis of extra phase-pure $Li_4Ti_5O_{12}$ spinel," *Science of Sintering*, vol. 43, no. 3, pp. 343–351, 2011.

[16] A. Nugroho, S. J. Kim, K. Y. Chung, B.-W. Cho, Y.-W. Lee, and J. Kim, "Facile synthesis of nanosized $Li_4Ti_5O_{12}$ in supercritical water," *Electrochemistry Communications*, vol. 13, no. 6, pp. 650–653, 2011.

[17] J. Lim, E. Choi, V. Mathew et al., "Enhanced high-rate performance of $Li_4Ti_5O_{12}$ nanoparticles for rechargeable Li-ion batteries," *Journal of the Electrochemical Society*, vol. 158, no. 3, pp. A275–A280, 2011.

[18] S. C. Lee, S. M. Lee, J. W. Lee et al., "Spinel $Li_4Ti_5O_{12}$ nanotubes for energy storage materials," *Journal of Physical Chemistry C*, vol. 113, no. 42, pp. 18420–18423, 2009.

[19] C. M. Julien, M. Massot, and K. Zaghib, "Structural studies of $Li_{4/3}Me_{5/3}O_4$ (Me = Ti, Mn) electrode materials: local structure and electrochemical aspects," *Journal of Power Sources*, vol. 136, no. 2, pp. 72–79, 2004.

[20] I. A. Leonidov, O. N. Leonidova, L. A. Perelyaeva, R. F. Samigullina, S. A. Kovyazina, and M. V. Patrakeev, "Structure, ionic conduction, and phase transformations in lithium titanate $Li_4Ti_5O_{12}$," *Physics of the Solid State*, vol. 45, no. 11, pp. 2183–2188, 2003.

[21] D. Z. Liu, W. Hayes, M. Kurmoo, M. Dalton, and C. Chen, "Raman scattering of the $Li_{1+x}Ti_{2-x}O4$ superconducting system," *Physica C: Superconductivity*, vol. 235-240, no. 2, pp. 1203–1204, 1994.

[22] R. Baddour-Hadjean and J.-P. Pereira-Ramos, "Raman microspectrometry applied to the study of electrode materials for lithium batteries," *Chemical Reviews*, vol. 110, no. 3, pp. 1278–1319, 2010.

[23] D. Li and H. Zhou, "Two-phase transition of Li-intercalation compounds in Li-ion batteries," *Materials Today*, vol. 17, no. 9, pp. 451–463, 2014.

[24] S. Scharner, W. Weppner, and P. Schmid-Beurmann, "Evidence of two−phase formation upon lithium insertion into the $Li_{1.33}Ti_{1.67}O_4$ spinel," *Journal of the Electrochemical Society*, vol. 146, no. 3, pp. 857–861, 1999.

[25] M. Vijayakumar, S. Kerisit, K. M. Rosso et al., "Lithium diffusion in $Li_4Ti_5O_{12}$ at high temperatures," *Journal of Power Sources*, vol. 196, no. 4, pp. 2211–2220, 2011.

[26] D. V. Safronov, S. A. Novikova, A. M. Skundin, and A. B. Yaroslavtsev, "Lithium intercalation and deintercalation processes in $Li_4Ti_5O_{12}$ and $LiFePO_4$," *Inorganic Materials*, vol. 48, no. 1, pp. 57–61, 2012.

[27] A. J. Bard and L. R. Faulkner, *Electrochemical Methods and Applications*, Wiley-Interscience, New York, NY, USA, 2000.

[28] Y. Shi, L. Wen, F. Li, and H.-M. Cheng, "Nanosized $Li_4Ti_5O_{12}$/graphene hybrid materials with low polarization for high rate lithium ion batteries," *Journal of Power Sources*, vol. 196, no. 20, pp. 8610–8617, 2011.

[29] Y. Li, G. L. Pan, J. W. Liu, and X. P. Gao, "Preparation of $Li_4Ti_5O_{12}$ nanorods as anode materials for lithium-ion batteries," *Journal of the Electrochemical Society*, vol. 156, no. 7, pp. A495–A499, 2009.

[30] D. K. Lee, H.-W. Shim, J. S. An et al., "Synthesis of heterogeneous $Li_4Ti_5O_{12}$ nanostructured anodes with long-term cycle stability," *Nanoscale Research Letters*, vol. 5, no. 10, pp. 1585–1589, 2010.

[31] N. Cao, L. Wen, Z. Song et al., "$Li_4Ti_5O_{12}$/reduced graphene oxide composite as a high-rate anode material for lithium ion batteries," *Electrochimica Acta*, vol. 209, pp. 235–243, 2016.

[32] B. Li, F. Ning, Y.-B. He et al., "Synthesis and characterization of long life $Li_4Ti_5O_{12}$/C composite using amorphous TiO_2 nanoparticles," *International Journal of Electrochemical Science*, vol. 6, pp. 3210–3223, 2011.